Probe Measurements of the Discharge in an Operating Electron Bombardment Engine

WILLIAM B. STRICKFADEN* AND KENNETH L. GEILER*
Jet Propulsion Laboratory, California Institute of Technology, Pasadena, Calif.

Current-voltage characteristics have been obtained from Langmuir probes at various positions inside a Kaufman-type ion motor. Data are presented for the engine in static (no beam, but plasma) and operating (160-ma beam) conditions. The analysis of the probe data indicates that the electrons in the plasma possess a non-Maxwellian distribution of energies. To obtain plasma properties from the probe curves, the non-Maxwellian energy distribution is assumed to consist of a primary monoenergetic group of high-energy electrons plus the usual Maxwell distribution. Based upon this assumption, the probe curves are analyzed for primary and Maxwell energies and densities, and the data for radial positions inside the engine are presented. It is shown from the density curves that the primary electrons are the principal source of ion production. The beam current as calculated from probe data near the exit grids agrees to the correct order of magnitude with the measured value.

Introduction

THE possibilities of the Kaufman-type[1] electron bombardment ion source for use as a thrust device for deep-space applications is well documented.[2] Even though the engine in its present state achieves reasonable efficiencies, its operation is not understood thoroughly. The engine always has been studied externally; the variation of beam current, propellant utilization efficiency, etc., have been measured as one changes the various external operating parameters such as arc voltage and magnetic field. For a deeper understanding of the source operation, it is necessary to probe the interior of the engine, where the plasma is being formed. Only in this way can one correlate a theoretical model to the actual situation. Then, if a proper model can be found, a calculation of the efficiencies and beam properties hopefully can be made from the operating parameters, and it will be possible to try to improve the engine operation for its ultimate use as a thrust device.

This paper deals with an experimental program set up to investigate the properties of the plasma inside an operating Kaufman-type engine. From the results of this investigation, it is hoped that a theoretical model can be developed which will explain plasma formation sufficiently so that future engines of this type can be built with predictable characteristics.

Because of their small size and ability to distinguish plasma properties at different points, Langmuir probes[3] were used to probe the inside of the engine. These probes are simple to operate and need a minimum amount of circuitry, advantages not to be overlooked when the engine is operated under flight-simulated conditions during which the whole device is floating at a potential of about 5 kv.

Experimental Setup

For this investigation, an ion engine of the Kaufman type was purchased from Goodrich-High Voltage Astronautics, Inc.† A schematic diagram of this engine and associated power supplies is given in Fig. 1.

The propellant, mercury, enters the arc or discharge chamber as a gas through a distributor in the rear of the engine. A cylindrical, nickel matrix oxide, indirectly heated cathode is positioned along the axis of the engine. A cylindrical anode surrounds the cathode and is attached to, but electrically isolated from, the engine housing. The accelerator electrodes consist of two 0.060-in. molybdenum plates through which a matrix of 0.187-in. holes has been drilled in a close-pitch hexagonal array. One of the electrodes is attached to and is electrically common with the engine housing that forms the arc chamber. The second electrode is mounted downstream of the first on three ceramic insulators. A solenoidal magnet is wound around the entire housing to provide field divergence downstream of the accelerating electrodes. A decelerating electrode is not employed.

During engine operation, the housing, cathode sheath, magnet, and propellant feed system are electrically common and maintained at high positive potential while the outer accelerating electrode is biased negatively, typically -1000 to -1500 v. The anode remains positive with respect to the engine housing by the arc or discharge potential. The cathode temperature is varied to achieve a desired arc current for any selected arc voltage, thus insuring temperature-limited cathode operation.

The engine was installed in a 3- by 7-ft vacuum chamber capable of being evacuated to 10^{-7} mm Hg (Fig. 2). A cryogenically cooled collector was positioned 30 in. downstream of the engine-accelerating electrode. The collector is a two-section type, providing beam current measurements and suppression of secondary electrons.

A moveable Langmuir probe (Fig. 3) was constructed by encapsulating a 0.020-in.-diam pure tungsten wire within a 96% fused silica sheath packed with finely powdered boron nitride. The tungsten wire was allowed to protrude 0.300 in. from the end of the sheath.

The probe was inserted into the plasma from the rear of the engine through a boron nitride feed-through insulator and connected to a traversing and radial positioning mechanism located outside of the vacuum tank. This mechanism was designed and constructed to provide probe position information to a tolerance of ± 0.015 in. in both the axial and radial directions.

Probe instrumentation, which consisted of a 0- to 250-v-d.c. power supply, variable frequency function generator,

Presented at the AIAA Electric Propulsion Conference, Colorado Springs, Colo., March 11–13, 1963. This paper presents the results of one phase of research carried out at the Jet Propulsion Laboratory, California Institute of Technology, under Contract No. NAS 7-100, sponsored by NASA. The authors wish to acknowledge in particular the contributions of two of their colleagues: Roy W. Adams, for his patient and careful assistance in data collection, and Daniel J. Kerrisk, for his very illuminating discussions.

* Research Engineer, Advanced Propulsion Engineering Section.

† Now Ion Physics Corporation, a subsidiary of High Voltage Engineering Corporation, Burlington, Mass.

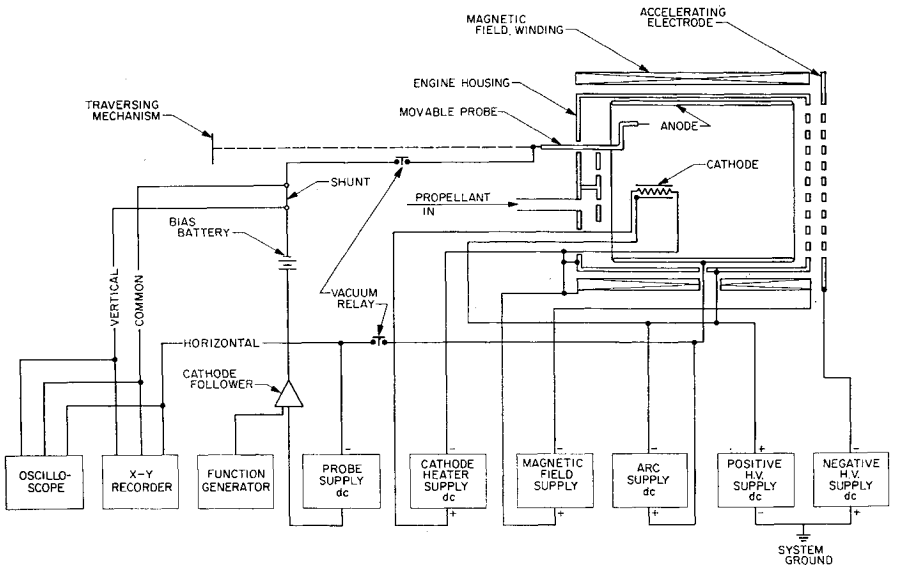

Fig. 1 Circuit diagram of engine and probe.

cathode follower amplifier, x-y plotter with an input impedance of 1 meg, oscilloscope, bias batteries, and 100-ohm shunt, was connected together electrically as illustrated in Fig. 1. The instrumentation was isolated from ground potential and coupled to the ion engine and probe through two high-voltage vacuum relays, thus providing instrumentation decoupling capability without disturbing engine operation. All probe voltage information was referenced to anode potential.

A second Langmuir probe of variable area (Fig. 4) was constructed, for reasons discussed later in this paper. This probe consisted of a 0.090-in.-diam pure tungsten rod sheathed in a boron nitride insulator. One end of the tungsten rod was attached to a solenoid, which, when actuated, could vary the length of the rod protruding from the insulator. In the retracted position the rod protruded 0.050 in. from the insulator, whereas in the extended position the rod protruded 0.350 in. The probe was inserted into the plasma from the rear of the engine. No traversing mechanism was employed on the second probe.

Typical Results

The analysis of a Langmuir probe characteristic (LPC) is simple if the electrons in the plasma are distributed according to the Maxwell-Boltzmann law. In this case a plot of the LPC on semilogarithmic graph paper will yield a straight line.

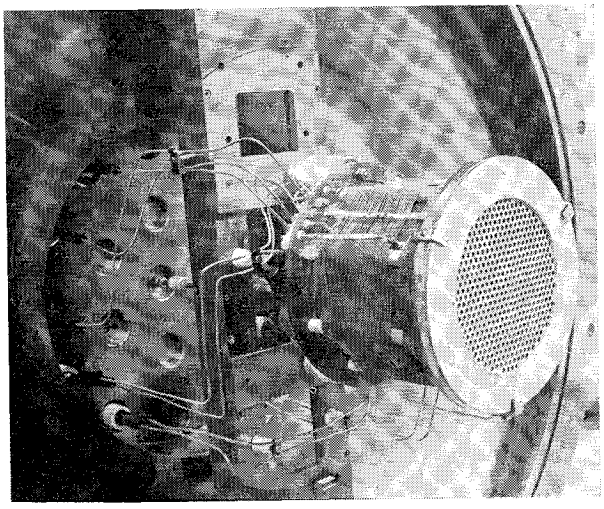

Fig. 2 View of experimental setup.

Quite early in this program many LPC's were obtained which did not plot as straight lines. Sometimes the deviation was small, sometimes large. In most cases the upper portion of the LPC was linear, the deviation from linearity not occurring until the probe was some 5 to 10 v below plasma potential. In such cases, the question arises as to whether the deviations are due to an actual non-Maxwellian energy distribution law, or to some external cause such as an improper circuitry or a probe surface contamination, or to one of the many other phenomena evoked by experimenters using Langmuir probes. A definite answer to the question is hard to give, but from a series of independent experiments (some to be described below) it appears that the anomalous LPC's are a result of a non-Maxwellian distribution law for the electrons in the plasma. It also will become apparent that the deviation from Maxwellian may be quite important in determining the operation of the source. A similar non-Maxwellian distribution has been reported by other workers, notably Medicus,[4] who studied a fireball discharge in neon.

Figure 5 presents a typical semilogarithmic plot of an LPC taken with the moveable probe. Note the deviation from a straight line at negative values of the voltage. This type of behavior is typical of most of the LPC's taken under various operating conditions inside the engine. However, if the arc voltage is low enough, as shown in Fig. 5, the LPC follows a straight line for three decades of the current.

It is known that for some plasmas an anomalous characteristic such as that shown in Fig. 5 is found when the plasma creeps up the insulator of the probe for increasing negative voltages. To show that the anomalous LPC's do

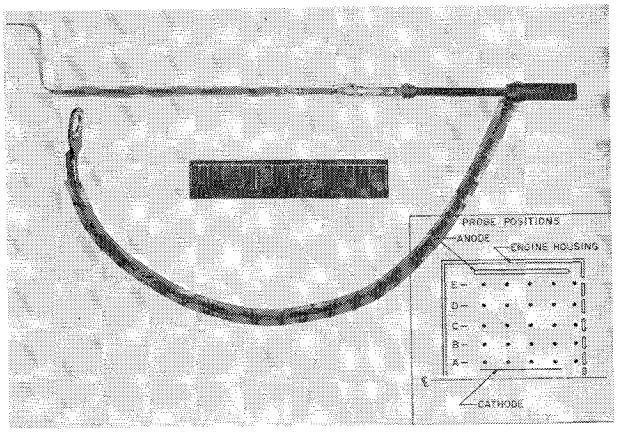

Fig. 3 Moveable probe; insert shows approximate probe positioning points inside engine.

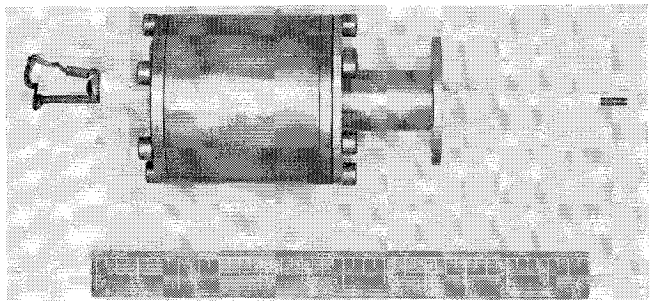

Fig. 4 Variable area probe.

not occur from some probe-insulator-plasma interaction, the variable-area probe described previously was used. Figure 6 illustrates the results. The curve labeled "extended" is the LPC obtained by the probe in the extended position; any probe-insulator interaction should be present in this curve. The curve labeled "difference" is the difference between the two LPC's obtained by the probe in the extended and retracted positions; any insulator effect should not appear in the "difference" curve. A comparison of the "extended" and "difference" curves shows no difference, thus ruling out any effect of insulator-plasma interaction on the probe traces.

To show that the anomalous LPC's do not result from the formation of oxides, amalgams, or other contamination of the probe surface, the voltage on the probe was driven to high positive values. By sweeping the voltage on the probe at 0.01 cps, electron currents large enough to heat the probe to incandescence could be maintained for some tens of seconds. Heating by electron bombardment should raise the surface temperature of the probe high enough to boil off any contaminants. It was found that LPC's taken with a probe immediately after cleaning in the foregoing manner were identical to those taken when the probe was not heated to incandescence.

From the preceding discussion, it is seen that the anomalous LPC's probably are due to an actual non-Maxwellian energy distribution for the electrons. Since the LPC at any voltage V is an integral of the energy distribution taken from the energy eV to infinity, an excess of high-energy electrons in the distribution would yield an LPC of the type observed. This interpretation is made throughout the remainder of this paper. Quantitative evaluation of the probe curves will be made in the next section.

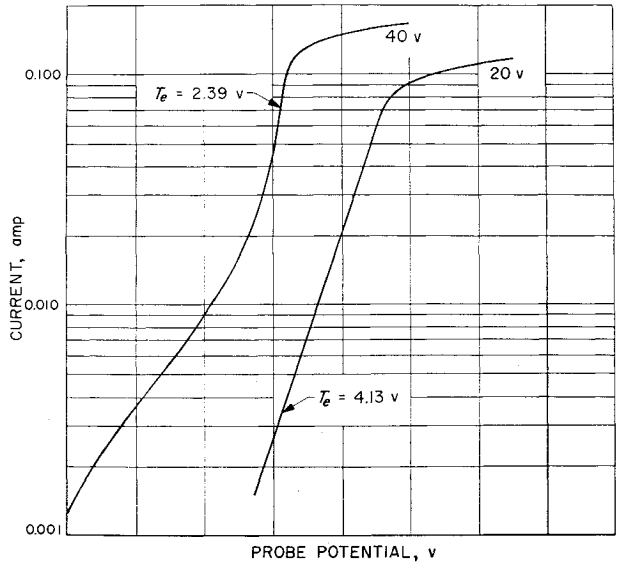

Fig. 5 Typical semilogarithmic LPC showing variation in probe trace with arc voltage (arc voltage, noted; magnetic field, 20 gauss, 6 amp; arc current, 2 amp; flow rate, 1.7 g/hr).

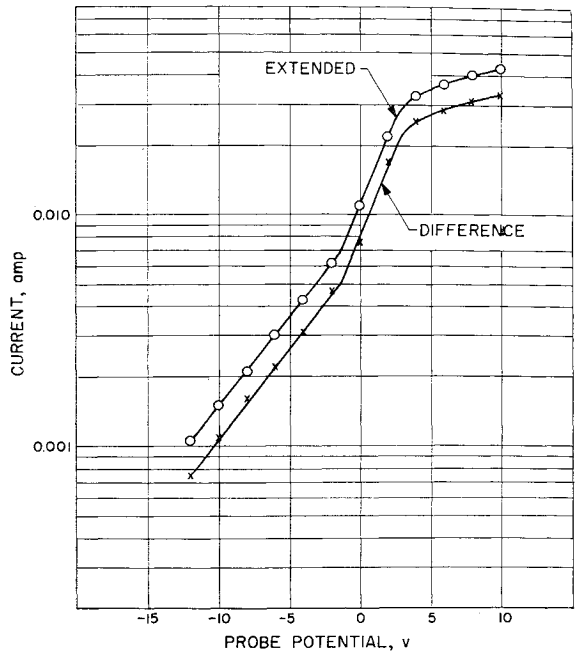

Fig. 6 Typical semilogarithmic LPC from variable area probe (arc voltage, 20 v; magnetic field, 10 gauss, 3 amp; arc current, 0.85 amp; flow rate, 1.7 g/hr).

Figure 7 shows five LPC's taken at different radial positions in the engine. The engine operating parameters are noted in the caption. Observe the gradual decrease in electron saturation current and general straightening of the curves near the anode. The saturation current is an approximate measure of the density of electrons which, as expected, decreases radially. This type of behavior is typical of all the LPC's obtained under many different operating conditions and was observed very near the grids when accelerating voltage was on or off.

Under some operating conditions severe "hash" in the saturated electron current portion of the LPC's was observed when the characteristic was viewed on an oscilloscope. This "hash" is interpreted as some sort of plasma oscillations and could be observed by coupling the oscilloscope to any portion of the engine. Figures 8 and 9 illustrate an example of the magnitude of these oscillations. The only difference be-

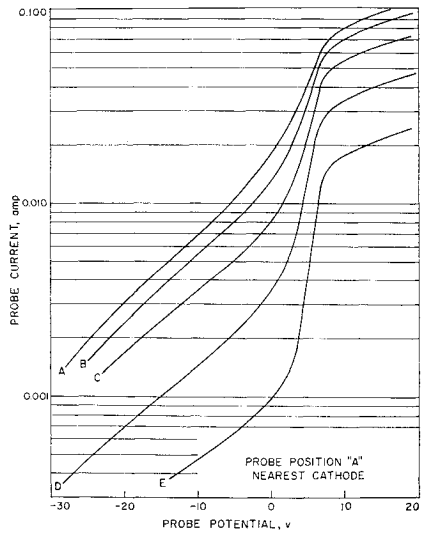

Fig. 7 Typical radial semilogarithmic LPC's (arc voltage, 50 v; magnetic field, 14 gauss, 4 amp; arc current, 2 amp; flow rate, 1.7 g/hr).

tween the two pictures is the magnetic field intensity. Figure 8 was taken at 20 gauss, Fig. 9 at 25 gauss. These strong oscillations always were present above a certain critical field strength and may play an important role in engine operation. Since the LPC's to be used for analysis were taken with an x-y recorder, no meaningful traces could be obtained when the strong oscillations were present. Therefore, it was not possible to obtain any information on the plasma when the magnetic field was above about 20 gauss.

Analysis of LPC

In order to obtain useful information on the plasma, a method of breaking down the LPC into an energy distribution for the electrons was devised. Before detailing this method, some general criteria will be presented showing the applicability of Langmuir probes to investigations of plasma of the kind found in the Kaufman engine:

1) For the probe to act like an infinite planar probe, the sheath thickness should be small in comparison to the size of the probe. For a current density of 0.004 amp/cm^2 and a voltage of 21.5 v, the sheath will be 9.8×10^{-3} cm, as calculated by the space charge equation, which is much smaller than the diameter of any of the cylindrical probes used.

2) Elementary probe theory assumes that there are very few collisions in the sheath. This means that the sheath must be small in comparison to the mean free path of the electrons. In the Kaufmann engine, particle densities are of the order of 10^{11} particles/cm^3, which gives a mean free path of several meters—much larger than the sheath indeed.

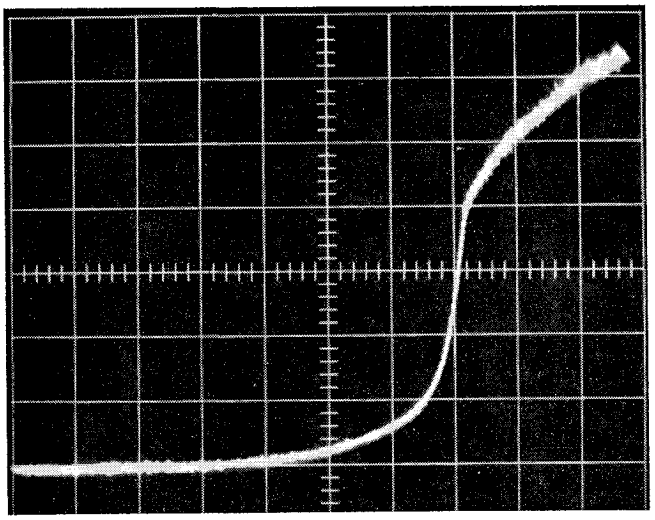

Fig. 8 Typical LPC obtained on oscilloscope (arc voltage, 40 v; magnetic field, 20 gauss, 6 amp; arc current, 2 amp; flow rate, 1.7 g/hr).

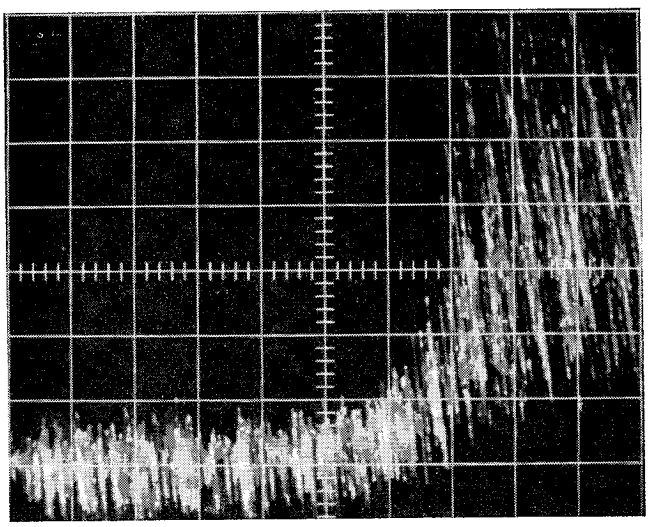

Fig. 9 Typical LPC obtained on oscilloscope showing oscillations (arc voltage, 40 v; magnetic field, 25 gauss, 9 amp; arc current, 2 amp; flow rate, 1.7 g/hr).

3) Since the probe is collecting electrons in the magnetic field of the engine, the effect of the magnetic field upon collection either must be corrected for or must be small enough to be neglected. If the cyclotron radius of the electrons is large compared to the probe dimensions, the effect of the magnetic field will be small. The cyclotron radius for a 5-ev electron in a 20-gauss field is 0.3 cm, which is large compared to the probe diameter of 0.05 cm.

From these data it is clear that the usual infinite planar probe theory will be applicable.

When the plasma electrons possess a Maxwell distribution of energies, the current to an infinite planar probe for voltages negative with respect to the plasma potential is‡

$$i = AeN_m(kT_e/2\pi M_e)^{1/2} \exp(-eV/kT_e) \tag{1}$$

where

A = area of probe
e = electronic charge
N_m = number of Maxwell electrons
k = Boltzmann's constant
T_e = electron temperature
M_e = mass of the electron
V = $V_S - V_0$
V_S = plasma potential
V_0 = potential applied to probe

When the probe is at plasma potential, $V = 0$, and the saturation electron current i_{sm} is

$$i_{sm} = AeN_m(kT_e/2\pi M_e)^{1/2} \tag{2}$$

From (1), the current-voltage curve will plot as a straight line on semilogarithmic graph paper, and the electron temperature can be determined from the slope of this line. The plasma potential can be found from the breakpoint in the current-voltage curve. Knowing the plasma potential and the electron temperature, the density of the Maxwell electrons can be found using (2).

Now consider the case of a monoenergetic group of electrons of number N_p and energy E_p. Assume random orientated velocities in space. The current to an infinite planar probe now is [Ref. 5, p. 1243, Eq. (5)]

$$i_p = (AeN_p/4)(2eV_p/M_e)^{1/2}[1 - (V/V_p)] \tag{3}$$

where V_p is the electron-volt energy equivalent of E_p. Thus, in this case, the current-voltage probe curves will be linear. Again, at plasma potential, when $V = 0$,

$$i_{sp} = (AeN_p/4)(2eV_p/M_e)^{1/2} \tag{4}$$

and, since V_p can be determined from the current-voltage curve, N_p can be found from (4).

Figure 10 shows a typical anomalous LPC on a linear scale. Note that, for large negative voltages, the curve can be approximated by a straight line corresponding to monoenergetic electrons of an energy of approximately 22 v. When the straight line indicated is subtracted from the original data, the remaining curve plots as a straight line on a semilogarithmic plot. Figure 11 shows the original data on a semilogarithmic plot together with the remaining curve after the straight line has been subtracted. It is seen that the electron energy distribution leading to the anomalous-type

‡ Actually, one should analyze only the electron current to the probe. That is, use $i_e = i + |i_+|$, where i_e is the electron current, i is the probe current, and i_+ is the saturated ion current. Since $i_+ \ll i$ for most of the voltage ranges considered, the probe current always has been used instead of the electron current for the analysis.

LPC may be approximated by a distribution of electrons composed of two parts: 1) a "primary" distribution of monoenergetic electrons of high energy with randomly oriented velocities, and 2) a Maxwell distribution of electrons with a low mean energy.

The foregoing energy distribution is not an unreasonable distribution to assume for the electrons in the plasma. The primary electrons are those electrons from the cathode which are accelerated through the cathode sheath and undergo no collisions. The magnetic field of the engine will produce a random distribution of velocities. Inelastic collisions of the primary electrons with neutral atoms will produce electrons with a Maxwell energy distribution.

Electron-electron and electron-atom elastic collisions will tend to produce a spread in the energy of the primary distribution. One would expect the primary energy distribution to be represented better as Gaussian of half-Gaussian than as the monoenergetic spike used in the foregoing. Thus, the current-voltage probe curves would not be exactly straight lines at large negative voltages, but a more complicated function, approximating a straight line as the Gaussian becomes narrower.

All of the data taken were analyzed by using the monoenergetic-plus-Maxwell energy distribution approximation, even though in some cases the current-voltage curves were far from linear at negative probe voltages. It must be emphasized that the assumed distribution is only an approxi-

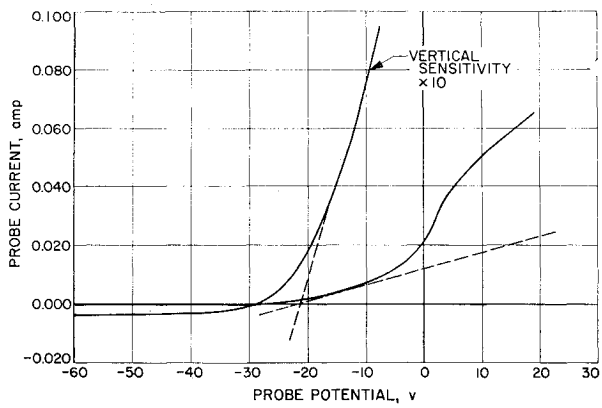

Fig. 10 Typical LPC from *x-y* recorder (linear scale) (arc voltage, 30 v; magnetic field, 16 gauss, 5 amp; arc current, 1.5 amp; flow rate, 1.6 g/hr).

mation to reality and is used at this time because of its simplicity in application. A better method would be to compute the energy distribution directly from the LPC as Druyvesteyn[6] and Medicus[5] did, but this method involves taking second derivatives of the characteristics, which is a highly inaccurate and tedious procedure.

Results

The results of applying the foregoing analysis to the radial probe traces for two sets of operating conditions are shown in Figs. 12 and 13. The operating conditions were identical in the two cases, except that in Fig. 13 the engine was producing a 160-ma beam. Therefore, the figures show a comparison of the plasma under operating and static conditions. All of the plasma properties obtained from the probe curves have been plotted on these figures except the plasma potential, which was very difficult to measure. The plasma potential usually varied between 2 to 7 v above anode potential. The accuracy of these curves is estimated at only about 30%, the large error being due mostly to the straight-line approximation to the primary electrons. Even so, the trend can be determined.

It is seen that the density of primary electrons drops off almost linearly with radial distance, whereas the Maxwell density usually drops much more slowly. There is also a definite drop in electron temperature in the radial direction. The drop in the electron temperature may be explained if there is significant energy exchange between the electrons of the primary and Maxwell groups. Since the primary and

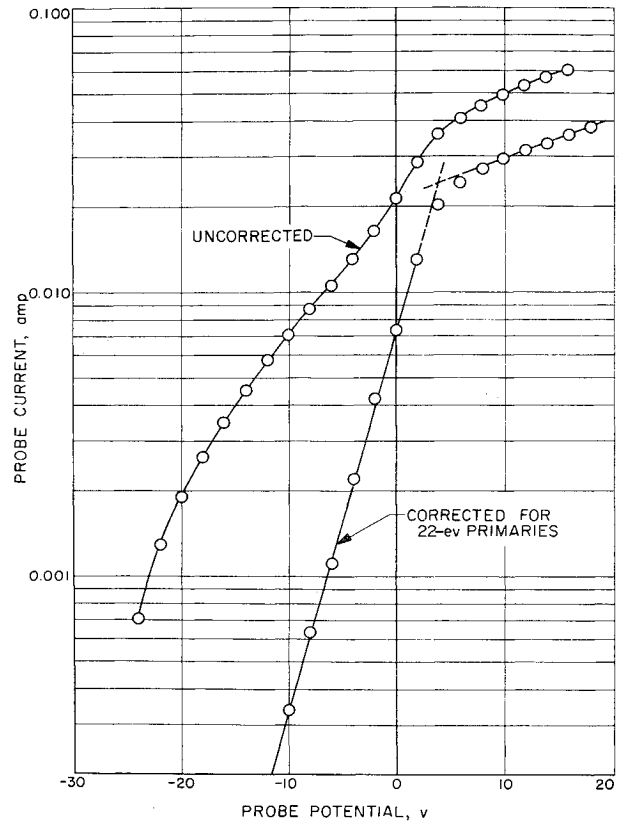

Fig. 11 Corrected and uncorrected semilogarithmic LPC (operating conditions same as for Fig. 10).

Maxwell densities are larger near the center of the engine, the greatest energy exchange between the groups would occur there, and since the energy of the primary electrons is higher than the Maxwell, the Maxwell mean energy would be raised.

The number density of ions was not measured, but if the plasma is assumed electrically neutral, the number of ions should equal the total number of electrons. This number also falls off with radial distance, most often following the density of Maxwell electrons, since the ratio of Maxwell to primary electrons is usually low. In fact, in a few cases the density of Maxwell electrons was found to increase going out from the cathode, approach a maximum about halfway between anode and cathode, and then fall off quite rapidly. The Maxwell electrons (and therefore the ions) were concentrated in an annular ring about the cathode.

The effect of applying accelerating voltage is seen to reduce the density of Maxwell electrons, at the particular radial position at which the radial traces were taken, which drastically increases the ratio of primary to Maxwell electrons. It is not clear why the accelerating potential should cause such an effect. One would expect that the plasma near the grids would shield the interior plasma quite effectively, but evidently this is not the case. The extraction of ions through the grids must set up axial electric fields that alter the spatial distribution of the lower-energy Maxwell electrons. The axial spatial distributions taken from axial sweeps of the Langmuir probe (data not shown here) do, in fact, show a gross rearrangement of the Maxwell electrons when high voltage is applied.

To see the effect of the primary electrons upon plasma formation, consider

$$\dot{N}_+(r,E) = dN_+(r,E)/dt$$

the rate of production of positive ions at any point, r, by electrons of energy E. This is given by

$$\dot{N}_+(r,E) = N_0(r)f(E,r)\sigma_i(E)v \qquad (5)$$

where

$N_0(r)$ = number density of neutral atoms at point r
(E,r) = number of electrons with energy E at point r, i.e., spatial energy distribution of electrons
$\sigma_i(E)$ = cross section for ionization of a neutral atom
v = velocity of the electron

Assume that the energy distribution of electrons is made up of two parts, a primary and a Maxwell part, so that f can be written as

$$f(E,r) = f_p(E)N_p(r) + f_m(E)N_m(r) \qquad (6)$$

where the subscript p stands for primary and m for Maxwell; N_p and N_m are the spatial number density distributions; and f_p and f_m are the energy distributions. For the primary energy distribution, assume a monoenergetic distribution at an energy E_p. Then,

$$f_p(E) = \delta(E_p) \equiv \text{Dirac } \delta \text{ function} \qquad (6')$$

The rate of ion production at point r is determined by integrating (5) over all energies, using the energy distribution (6), (6'), and the usual Maxwell energy distribution:

$$\dot{N}_+(r) = \left(\frac{2}{m}\right)^{1/2} \int_0^\infty N_0(r)[f_p(E)N_p(r) + f_m(E)N_m(r)]\sigma_i(E)E^{1/2}dE$$

This yields on integration

$$\dot{N}_+(r) = (2/m)^{1/2}\sigma_m N_1 N_0(r) N_{pn}(r) E_p^{1/2}[Q_p(r) + Q_m(r)] \qquad (7)$$

where

m = electron mass
σ_m = maximum value of the electron-mercury ionization cross section
N_1 = N_p/N_{pn} = maximum value of primary density
$N_{pn}(r)$ = normalized primary density
E_p = energy of primary electrons
$Q_p(r)$ = $\sigma_n[E_p(r)/V_i]$
= normalized ionization cross section of mercury; approximation of σ_n used was developed by Kerrisk[2, 7] and is shown in Fig. 14

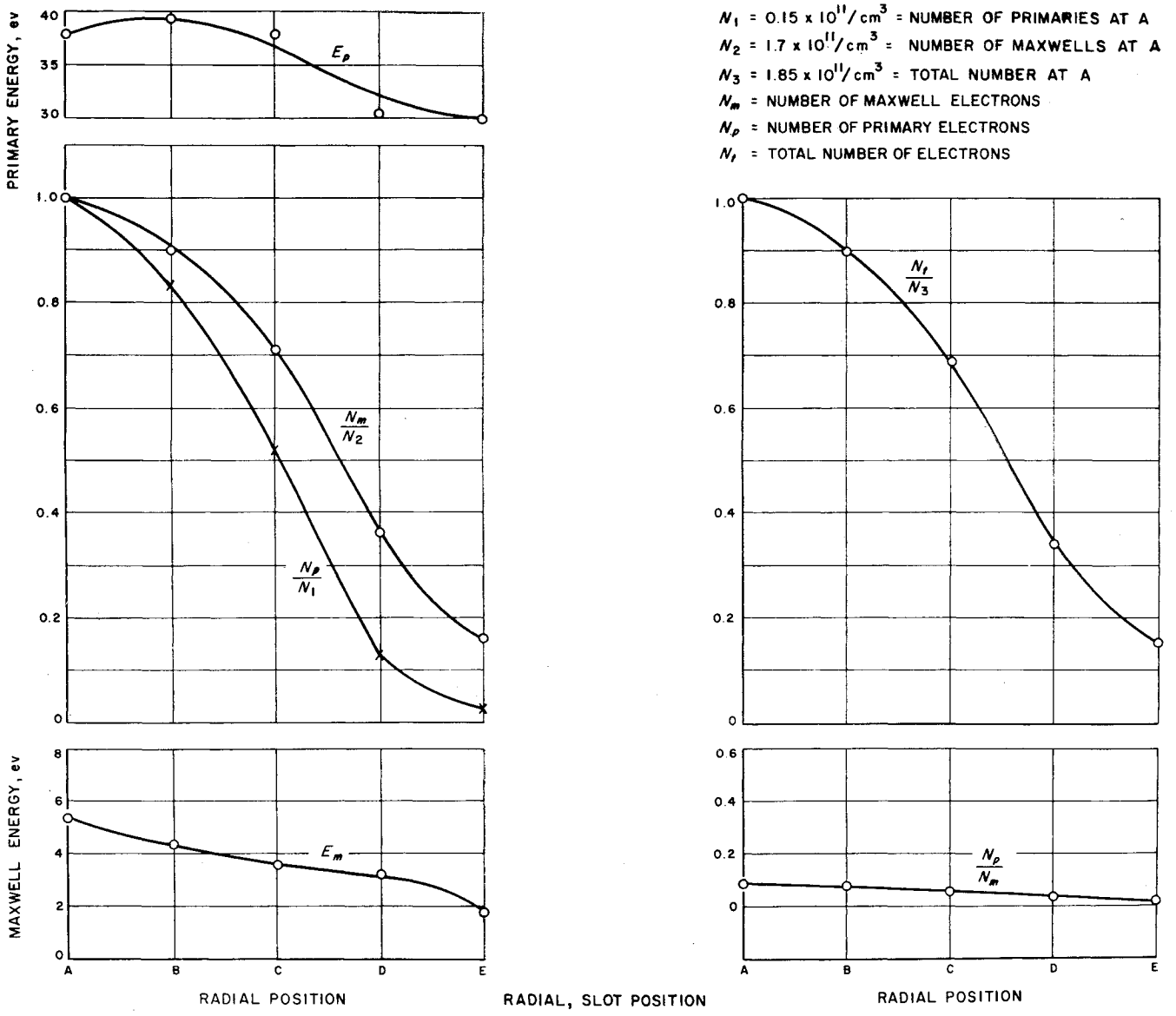

Fig. 12 Radial plot of electron density and energy variations (no accelerating potential applied) (arc voltage, 50 v; magnetic field, 20 gauss, 6 amp; arc current, 4 amp; flow rate, 1.5 g/hr).

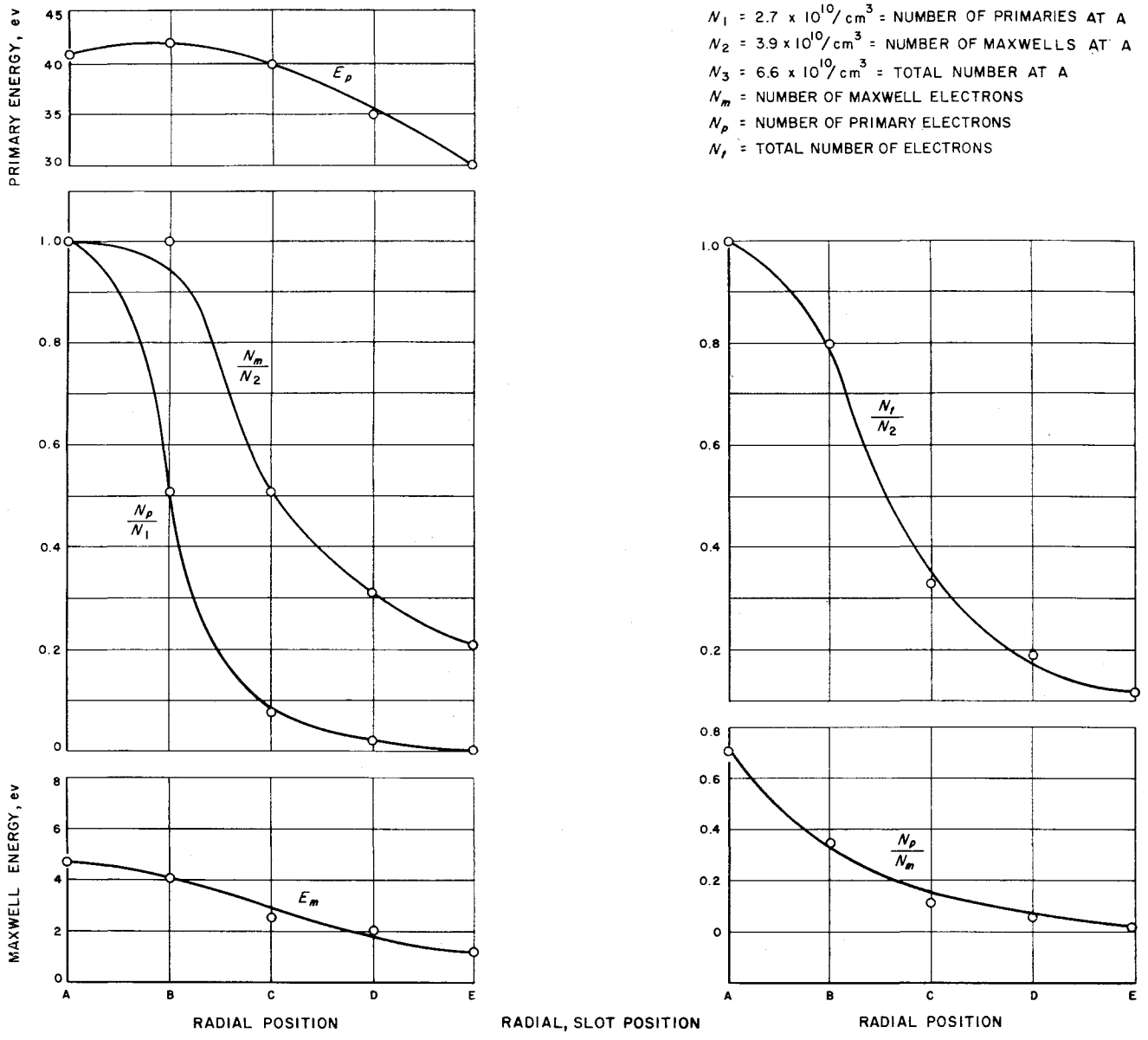

Fig. 13 Radial plot of electron density and energy variations (accelerating potential applied) (arc voltage, 50 v; acceleration voltage, 5 kv; arc current, 4 amp; engine beam current, 160 ma; magnetic field, 20 gauss, 6 amp; bias voltage, 1 kv; flow rate, 1.5 g/hr; interception current, 0.8 ma).

and where

$$Q_m(r) = \left(\frac{N_m}{N_p}\right)\left(\frac{E_m}{E_p}\right)^{1/2}\int_0^\infty f_m \sigma_n E^{1/2} dE$$

$$= \left(\frac{N_m}{N_p}\right)\left(\frac{E_m}{E_p}\right)^{1/2} P_m\left(\frac{E_m}{V_i}\right)$$

where

$P_m(E_m/V_i)$ = ionization coefficient of Maxwell electrons; this function has been evaluated by Kerrisk and is reproduced in Fig. 15
E_m = mean Maxwell energy
V_i = first ionization potential of mercury

Note that the functions Q_p and P_m will have a radial variation only if E_p and E_m vary radially. The functions Q_p and Q_m of Eq. (7) have been calculated from the spatial density distribution curves of Figs. 12 and 13 and are shown plotted in Figs. 16 and 17. One sees immediately that, even though there are fewer primary than Maxwell electrons, the function $Q_m(r)$ is at most $\frac{1}{10}$ as large as the function $Q_p(r)$. Furthermore, Q_m is a sensitive function of the Maxwell mean energy, and, since the mean energy always falls off in the radial direction, the ratio of Q_m to Q_p will be smaller at the anode than it is at the cathode. In other words, under most conditions, the term Q_m in Eq. (7) can be neglected in comparison to Q_p. It follows that the primary electrons are more effective in producing ions.

The ion current density J_+ necessary to form a stable sheath is given by Bohm[8] to be

$$J_+ = eN_+(kT_e/M_+)^{1/2} \quad (8)$$

If it is assumed that this equation is valid in the extraction region of the engine near the grids, then, from the measured values of the total ion density (N_+) and mean Maxwell energy (T_e), the ion current can be calculated. The calculation has been performed on the probe data obtained when the engine was producing a 160-ma beam with agreement to the correct order of magnitude. At the grids the current density near the anode was about $\frac{1}{7}$ the current density near the center of the engine at the grids.

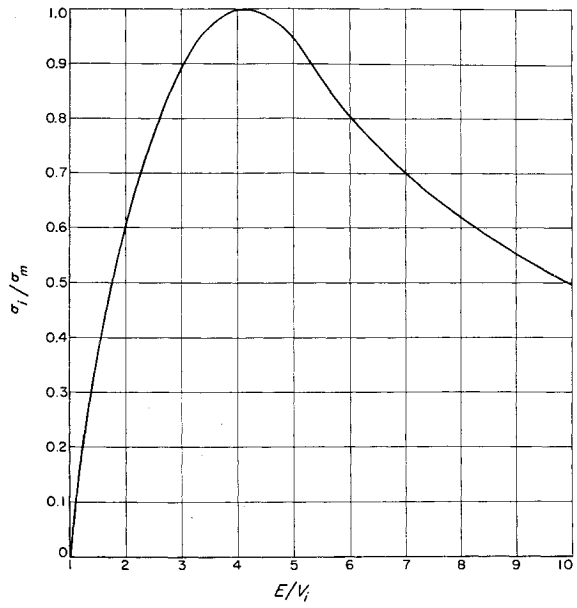

Fig. 14 Approximation of the mercury ionization cross section.

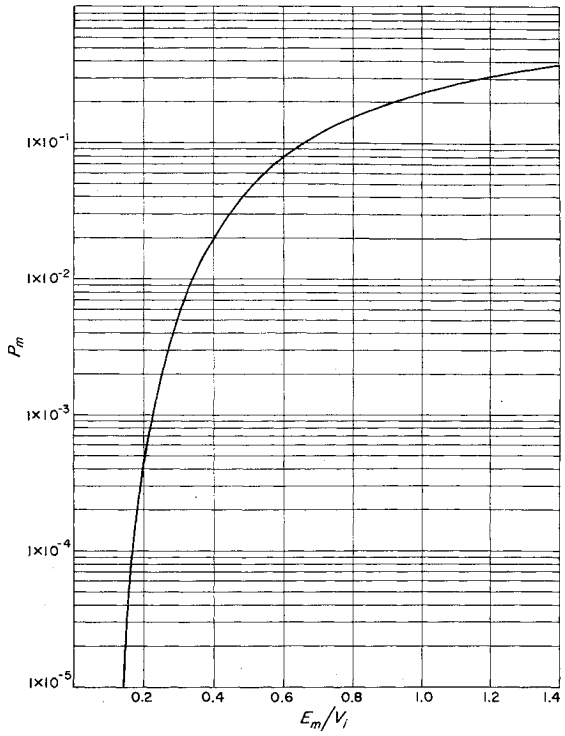

Fig. 15 Ionization coefficient for Maxwell electrons.

All of the data presented in this section are intended to be representative of a large amount of data under various operating conditions obtained from the probe curves. All the probe data for the following variations in engine parameters yield essentially similar results for the shape of the spatial density distributions: arc voltage, 20 to 60 v; arc current, 0.85 to 4.7 amp; magnetic field, 13 to 23 gauss; cathode temperature, 950° to 1250°C; propellant flow rate, 1.65 to 2.2 g/hr; net acceleration voltage, 3 to 8 kv; bias voltage, 1 to 1.5 kv; and beam current, 40 to 300 ma. A forthcoming report will present detailed probe data for the engine under various operating conditions.

Conclusions

Langmuir probe curves analyzed for the electron energy distribution for an operating (160-ma beam) and static (no beam, but plasma) Kaufman-type ion engine show that the energy distribution is not entirely Maxwellian. The energy distribution was found to consist of a high-energy primary distribution and a lower-energy Maxwell distribution. The primary electrons appear to be the main source of ion production. Furthermore, the ion density near the grids as well as in the interior of the engine is not uniform. Any theoretical model of this source must include the primary distribution of electrons.

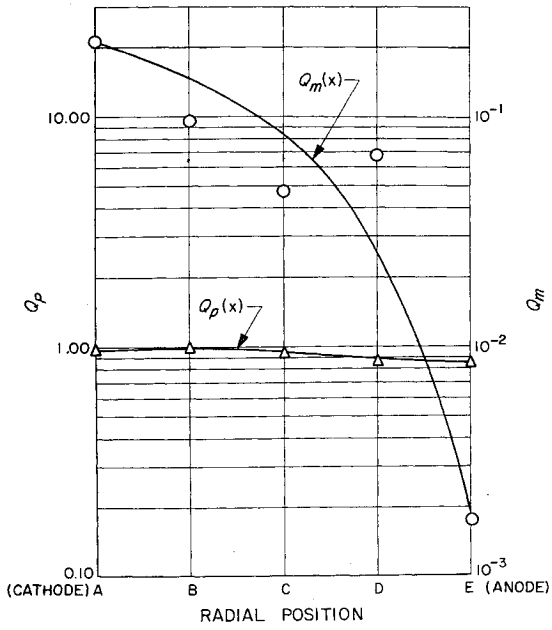

Fig. 16 Ionization rate curve (no accelerating potential applied) (operating conditions same as for Fig. 12).

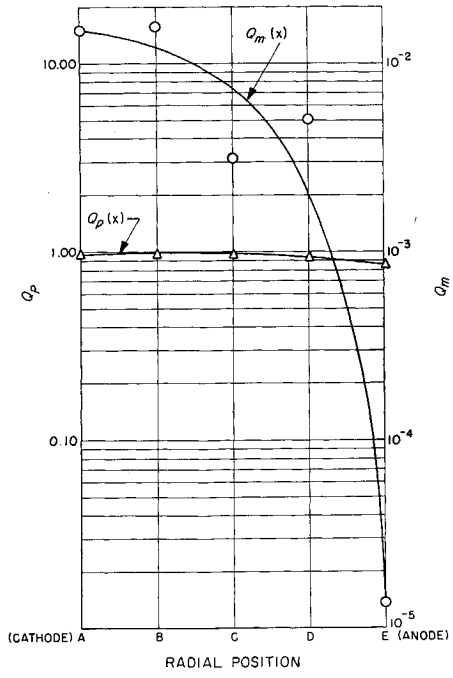

Fig. 17 Ionization rate curve (accelerating potential applied) (operating conditions same as for Fig. 13).

References

[1] Kaufman, H. R., "An ion rocket with an electron-bombardment ion source," NASA TN D-585 (1961).

[2] Kerrisk, D. J., "Potentialities of electron bombardment ion engines for electric propulsion," IRE Trans. Space Electron. Telemetry **8**, 188–193 (June 1962).

[3] Langmuir, I. and Mott-Smith, H. M., "The theory of col-

lectors in gaseous discharges," Phys. Rev. **28**, 727-763 (1926).

[4] Medicus, G., "Diffusion and elastic collision losses of the 'fast electrons' in plasmas," J. Appl. Phys. **29**, 903-908 (1958).

[5] Medicus, G., "Simple way to obtain the velocity distribution of the electrons in gas discharge plasmas from probe curves," J. Appl. Phys. **27**, 1242-1248 (1956).

[6] Druyvesteyn, M., "Der Neidervoltbogen," Z. Physik **64**, 781–798 (1930).

[7] Kerrisk, D. J., "Arc-type ion sources for electrical propulsion," TN 61-4, Aeronaut. Systems Div., Wright-Patterson Air Force Base (May 1961).

[8] Bohm, D., *Characteristics of Electrical Discharges in Magnetic Fields*, edited by A. Guthrie and R. K. Wakerling (McGraw Hill Book Co. Inc., New York, 1949), Chap. 3.

AUGUST 1963 AIAA JOURNAL VOL. 1, NO. 8

Concentrated Loads on Inflated Structures

LLOYD H. DONNELL*
Armour Research Foundation, Chicago, Ill.

The most efficient and practical mechanism for distributing concentrated loads into an inflated membranous envelope is a so-called "catenary curtain." This is a membranous strip attached to the envelope along one edge, whereas the other edge is scalloped, with the loads applied to the projecting points of the scallops. Such curtains have been used for transmitting the weight and other forces on the car of a nonrigid airship into the envelope, but these have been designed without consideration of the deformations involved. An analysis is presented of catenary curtains for applying normal or slightly oblique loads to an envelope. The relations between the forces and the changes in shape, displacements, and strains in the various elements of the curtain and the envelope are given, on the assumption that the curtain scallop spacing is small compared to the main dimensions of the envelope. The results are developed in the form of series that converge rapidly. They apply to relatively large displacements and unit strains up to the order of 0.1. Several examples are worked out.

Nomenclature

a,b,c = dimensions of catenary cable (Figs. 8 and 9)
b,f' = force per unit length between catenary curtain and envelope in direction of tie cable and normal to envelope surface
T,F = tension in catenary cable and its minimum value
0 = subscript indicating original value
p,p' = actual and "corrected" gas pressure in envelope, Eq. (7)
r,r' = radius of envelope before and after tensioning tie cable (Fig. 4)
u,u' = deflection of envelope in direction of tie cable and normal to envelope surface
W = tension in tie cable
x,y,s = coordinates of catenary cable perpendicular to, parallel to, and along cable
α,λ = angles between tie cable and envelope (Fig. 6)
β = $2b_0/a_0$
θ = $(b_1/b_0) - (1 + e_b)$
ϕ = $a(p'/F)^{1/2}$
$e_a,e_b,$ e_s,e_r = unit strains in a, b, s, and r

INFLATED structures, made of a tough membrane whose shape is maintained by a small internal pressure differential, have been used for many years. Because the pressure is small, they are insensitive to small leaks. They already have been used in space and are likely to be useful especially there because they make possible large structures of small weight, occupying little space before inflation.

All of the standard structural elements can be duplicated, for example, struts by inflated cylindrical tubes, but the chief application is in complete monocoque structures in which the membranous envelope provides both cover and structural stability. An important problem in connection with the design of such structures is that of applying concentrated loads to the envelope. Loads tangential to the envelope can be applied in a simple manner through patches, but these cause stress concentrations in the envelope which have been discussed by the author.[1, 2]

The most efficient and practical mechanism for distributing concentrated loads at any angle into the envelope is the so-called "catenary curtain." This is a membranous strip attached to the envelope along one edge, whereas the other edge is scalloped, with the loads applied through "tie-cables" to the projecting points of the scallops. The construction of a catenary curtain and the nomenclature that will be used are shown in Fig. 1.

Such curtains have been used for transmitting the weight and other forces on the car of a nonrigid airship into the envelope, but these have been designed without consideration of the deformations involved. This paper presents an analysis of catenary curtains for applying normal or slightly oblique loads to an envelope. It gives the relations between the forces and the changes in shape, displacements, and strains in the various elements of the curtain and envelope. This analysis can be used for calculating the change in shape produced by the elastic strains that occur when the structure is inflated initially, so as to allow for them in tailoring the curtain and the adjoining structure.

Since the membranous materials usually used are subject to plastic flow and creep, a more important application is likely to be to the problem of how the shape and load distribution will be affected by permanent strains due to yielding under overloads or to creep under normal loading over long periods of time. A study of the effect of permanent strains in a complete structure must take some account of the entire structure, but in such a study the catenary curtain presents special difficulties because of the complex relationship

Presented at the ARS 17th Annual Meeting and Space Flight Exposition, Los Angeles, Calif., November 13–18, 1962. This work was sponsored by General Development Corporation under a contract with the Bureau of Aeronautics, U. S. Navy.

* Staff Consultant; also Professor Emeritus of Mechanics, Illinois Institute of Technology, Chicago, Ill.